Tight focusing of partially polarized vortex beams by binary phase Fresnel zone plates*

Shu Jian-Hua(舒建华), Chen Zi-Yang(陈子阳),
Pu Ji-Xiong(蒲继雄)†, and Liu Yong-Xin(刘永欣)

College of Information Science and Engineering, Huaqiao University, Xiamen 361021, *China*

(Received 21 March 2011; revised manuscript received 18 May 2011)

Based on vectorial Debye theory, the focusing properties of partially polarized vortex beam by high numerical aperture Fresnel zone plate are investigated. The effects of the numerical apertures of and the phase difference of binary phase Fresnel zone plates, the topological charge of vortex beam and the degree of polarization of incident beam on the intensity distribution and degree of coherence in the focal plane are investigated in detail. It is shown that elliptical light spots and the flat top beam can be obtained by selecting certain parameters. Studies of degree of coherence reveal that the degree of coherence between x and y components of the electric field, which is zero in the source plane, is improved in the focal plane for vortex beam, but it is hardly changed for the nonvortex beam. It is also proved that any two of the three electric field components E_x, E_y and E_z are completely coherent everywhere in the focal region if the incident light beam is linearly polarized.

Keywords: partially polarized vortex beams, high numerical aperture, binary phase Fresnel zone plates

PACS: 42.25.Ja, 42.25.Fx **DOI:** 10.1088/1674-1056/20/11/114202

1. Introduction

In recent years, the focusing properties of the beams focused by a high numerical aperture (NA) objective have attracted much attention due to their potential applications in optical data storage, microscopy, material processing, the manipulation of particles etc.[1−6] Therefore, there has been much research on tight focusing of different kinds of beams, such as cylindrical vector beams, elliptical symmetry beams, linearly polarized beams and spirally polarized beams.[7−10] There are also a few papers concerning tight focusing of partially polarized vortex beams. Vortex beams carrying orbital angular momentum (OAM) have attracted many researchers due to their potential applications in optical information encoding and transmission, i.e., the topological charge associated with OAM of the vortex beams can be viewed as the information carrier.[11−16] In addition, a phase Fresnel zone plate (FZP) is an important focusing device especially in confocal microscopy and high resolution lithography.[17] Some interesting work about the use of binary phase FZP with a large NA has been reported in recent years.[18,19]

In the present paper, electromagnetic Laguerre–Gaussian (LG) beam is taken as an example to analyse the focusing properties of partially polarized vortex beam focused by a high NA phase FZP. We analyse the effects of the numerical apertures of and phase difference of binary phase FZPs, the topological charge of vortex beam and the degree of polarization of incident beam on intensity distribution and degree of coherence in the focal plane.

2. Theoretical model

We first consider the focusing of a linearly x-polarized beam by a high NA phase FZP. According to the classic paper by Wolf,[20] the electric field $E(r, \varphi, z)$ in the focal region can be expressed as[21]

$$E(r, \varphi, z) = \begin{bmatrix} E_x \\ E_y \\ E_z \end{bmatrix}$$

*Project supported by the National Natural Science Foundation of China (Grant No. 60977068), the Open Research Fund of Key Laboratory of Atmospheric Composition and Optical Radiation, Chinese Academy of Sciences (Grant No. SKLST200912), and the Overseas Chinese Affairs Office of the State Council (Grant No. 10QZR01).

†Corresponding author. E-mail: jixiong@hqu.edu.cn

$$= -\frac{\mathrm{i}kf}{2\pi}\int_0^{\alpha}\int_0^{2\pi} A(\theta,\phi)B(\theta)C(\theta)\sin\theta\exp(\mathrm{i}kz\cos\theta) \times \exp[\mathrm{i}kr\sin\theta\cos(\phi-\varphi)] \times \begin{bmatrix} \cos^2\phi\cos\theta+\sin^2\phi \\ \sin\phi\cos\phi(\cos\theta-1) \\ \sin\theta\cos\phi \end{bmatrix} \mathrm{d}\phi\mathrm{d}\theta, \quad (1)$$

where r, φ, and z are the cylindrical coordinates of an observation point, as shown in Fig. 1; $k(=2\pi/\lambda)$ is a wave vector; f is a focal length; $B(\theta)$ is a factor accounting for the energy conservation in the transmission of field through the focusing system; $C(\theta)$ is a phase transfer function; $A(\theta,\phi)$ is a pupil apodization function in the surface of phase FZP, which is related to the electric field of the incident beam.

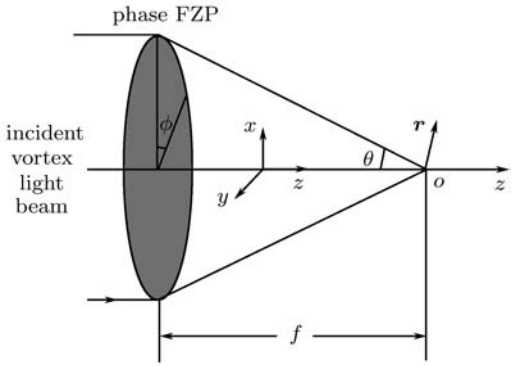

Fig. 1. Schematic diagram of the tight focusing system.

A partially polarized vortex beam can be simply expressed as the superposition of two orthogonal linearly polarized beams that have an uncertain and random phase difference, i.e.,

$$\boldsymbol{E}(\theta,\phi) = [A_x(\theta)\boldsymbol{e}_x + A_y(\theta)\boldsymbol{e}_y]\exp(\mathrm{i}m\phi), \quad (2)$$

where m is the topological charge of the vortex beam; $\boldsymbol{e}_x$ and $\boldsymbol{e}_y$ are unit vectors along the x and y directions, respectively; $A_x(\theta)$ and $A_y(\theta)$ are Cartesian components of the complex electric vector in the source plane. To illustrate the behaviour of the intensity distribution of partially polarized vortex beam in the focal region, we apply the theory to a particular case. We assume that the field amplitude in the source plane is of an LG mode and is expressed as

$$A_j(r) = E_j^0\left(\frac{\sqrt{2}r}{\omega_0}\right)^{|m|}\exp\left(-\frac{r^2}{\omega_0^2}\right), \quad j=x,y, \quad (3)$$

where E_j^0 $[=\left|E_j^0\right|\exp(\mathrm{i}\psi_j)]$ is the characteristic complex amplitude with a random phase ψ_j and ω_0 is the beam size in the source plane. Under the sine condition,[21] we have $r = f\sin\theta$ so that the pupil apodization function of the LG beam can be written as

$$A_j(\theta) = E_j^0\left(\frac{\sqrt{2}f\sin\theta}{\omega_0}\right)^{|m|}\exp\left(-\frac{f^2\sin^2\theta}{\omega_0^2}\right). \quad (4)$$

According to Eq. (1), the electric field in the focal region when a phase FZP is illuminated by partially polarized vortex beam can be calculated as

$$E(r,\varphi,z) = \begin{bmatrix} E_x \\ E_y \\ E_z \end{bmatrix} = -\frac{\mathrm{i}kf}{2\pi}\int_0^{\alpha}\int_0^{2\pi} B(\theta)C(\theta)\sin\theta\exp(\mathrm{i}kz\cos\theta)\exp[\mathrm{i}kr\sin\theta\cos(\phi-\varphi)] \times \begin{bmatrix} A_x(\theta)(\cos^2\phi\cos\theta+\sin^2\phi)+A_y(\theta)\sin\phi\cos\phi(\cos\theta-1) \\ A_x(\theta)\sin\phi\cos\phi(\cos\theta-1)+A_y(\theta)(\sin^2\phi\cos\theta+\cos^2\phi) \\ \sin\theta(A_x(\theta)\cos\phi+A_y(\theta)\sin\phi) \end{bmatrix} \exp(\mathrm{i}m\phi)\mathrm{d}\phi\mathrm{d}\theta. \quad (5)$$

Substituting Eq. (4) into Eq. (5), the x, y and z components of the electric field in the focal region can be simplified into

$$E_j(r,\varphi,z) = E_{xj}(r,\varphi,z) + E_{yj}(r,\varphi,z), \quad j=x,y,z, \quad (6)$$

where $E_{kj}(r,\varphi,z)$ $(k=x,y)$ is the j th component of the focused electric field generated by the k-component of the electric field of the incident beam. They can be expressed as

$$E_{xx}(r,\varphi,z) = -\frac{\mathrm{i}^{(1-m)}kf}{2}\int_0^{\alpha} A_x(\theta)B(\theta)C(\theta)\sin\theta\exp(\mathrm{i}kz\cos\theta)\{(1+\cos\theta) \times J_{-m}(kr\sin\theta)\exp(\mathrm{i}m\varphi)+\frac{1}{2}(1-\cos\theta)[J_{-(m+2)}(kr\sin\theta) \times \exp[\mathrm{i}(m+2)\varphi]+J_{-(m-2)}(kr\sin\theta)\exp[\mathrm{i}(m-2)\varphi]]\}\mathrm{d}\theta, \quad (7)$$

$$E_{yx}(r,\varphi,z) = -\frac{\mathrm{i}^{-m}kf}{4}\int_0^\alpha A_y(\theta)B(\theta)C(\theta)\sin\theta\exp(\mathrm{i}kz\cos\theta)(1-\cos\theta)\{J_{-(m+2)}(kr\sin\theta) \times \exp[\mathrm{i}(m+2)\varphi] - J_{-(m-2)}(kr\sin\theta)\exp[\mathrm{i}(m-2)\varphi]\}\mathrm{d}\theta, \quad (8)$$

$$E_{xy}(r,\varphi,z) = -\frac{\mathrm{i}^{-m}kf}{4}\int_0^\alpha A_x(\theta)B(\theta)C(\theta)\sin\theta\exp(\mathrm{i}kz\cos\theta)(1-\cos\theta)\{J_{-(m+2)}(kr\sin\theta) \times \exp[\mathrm{i}(m+2)\varphi] - J_{-(m-2)}(kr\sin\theta)\exp[\mathrm{i}(m-2)\varphi]\}\mathrm{d}\theta, \quad (9)$$

$$E_{yy}(r,\varphi,z) = -\frac{\mathrm{i}^{(1-m)}kf}{2}\int_0^\alpha A_y(\theta)B(\theta)C(\theta)\sin\theta\exp(\mathrm{i}kz\cos\theta)\{(1+\cos\theta) \times J_{-m}(kr\sin\theta)\exp(\mathrm{i}m\varphi) - \frac{1}{2}(1-\cos\theta)[J_{-(m+2)}(kr\sin\theta) \times \exp[\mathrm{i}(m+2)\varphi] + J_{-(m-2)}(kr\sin\theta)\exp[\mathrm{i}(m-2)\varphi]]\}\mathrm{d}\theta, \quad (10)$$

$$E_{xz}(r,\varphi,z) = -\frac{\mathrm{i}^{-m}kf}{2}\int_0^\alpha A_x(\theta)B(\theta)C(\theta)\sin^2\theta\exp(\mathrm{i}kz\cos\theta)\{J_{-(m+1)}(kr\sin\theta) \times \exp[\mathrm{i}(m+1)\varphi] - J_{-(m-1)}(kr\sin\theta)\exp[\mathrm{i}(m-1)\varphi]\}\mathrm{d}\theta, \quad (11)$$

$$E_{yz}(r,\varphi,z) = \frac{\mathrm{i}^{-(m-1)}kf}{2}\int_0^\alpha A_y(\theta)B(\theta)C(\theta)\sin^2\theta \times \exp(\mathrm{i}kz\cos\theta)\{J_{-(m+1)}(kr\sin\theta)\exp[\mathrm{i}(m+1)\varphi] + J_{-(m-1)}(kr\sin\theta) \times \exp[\mathrm{i}(m-1)\varphi]\}\mathrm{d}\theta. \quad (12)$$

The second-order coherence properties of partially polarized beam may be characterized by the 3×3 electric cross-spectral density matrix[22]

$$W(\boldsymbol{r}_1,\boldsymbol{r}_2,z) = \begin{bmatrix} W_{xx}(\boldsymbol{r}_1,\boldsymbol{r}_2,z) & W_{xy}(\boldsymbol{r}_1,\boldsymbol{r}_2,z) & W_{xz}(\boldsymbol{r}_1,\boldsymbol{r}_2,z) \\ W_{yx}(\boldsymbol{r}_1,\boldsymbol{r}_2,z) & W_{yy}(\boldsymbol{r}_1,\boldsymbol{r}_2,z) & W_{yz}(\boldsymbol{r}_1,\boldsymbol{r}_2,z) \\ W_{zx}(\boldsymbol{r}_1,\boldsymbol{r}_2,z) & W_{zy}(\boldsymbol{r}_1,\boldsymbol{r}_2,z) & W_{zz}(\boldsymbol{r}_1,\boldsymbol{r}_2,z) \end{bmatrix}, \quad (13)$$

where

$$W_{jk}(\boldsymbol{r}_1,\boldsymbol{r}_2,z) = \left\langle E_j^*(r_1,\varphi_1,z)E_k(r_2,\varphi_2,z)\right\rangle, \quad j,k = x,y,z, \quad (14)$$

r_1, r_2 and φ_1,φ_2 are the modulus and the angles of the transversal position vectors $\boldsymbol{r}_1$, $\boldsymbol{r}_2$ located in the observed plane respectively. The asterisk refers to the complex conjugate. Angle brackets denote an average monochromatic realization of the field. Substituting Eq. (6) into Eq. (14), we obtain

$$\begin{aligned} & W_{jk}(\boldsymbol{r}_1,\boldsymbol{r}_2,z) \\ = & \left\langle E_{xj}^*(r_1,\varphi_1,z)E_{xk}(r_2,\varphi_2,z)\right\rangle \\ & + \left\langle E_{xj}^*(r_1,\varphi_1,z)E_{yk}(r_2,\varphi_2,z)\right\rangle \\ & + \left\langle E_{yj}^*(r_1,\varphi_1,z)E_{xk}(r_2,\varphi_2,z)\right\rangle \\ & + \left\langle E_{yj}^*(r_1,\varphi_1,z)E_{yk}(r_2,\varphi_2,z)\right\rangle. \end{aligned} \quad (15)$$

Because the phase difference $(\psi_y - \psi_x)$ is uncertain and random for partially polarized beam, we have $\left\langle E_{xj}^*(r_1,\varphi_1,z)E_{yk}(r_2,\varphi_2,z)\right\rangle = \left\langle E_{yj}^*(r_1,\varphi_1,z)E_{xk}(r_2,\varphi_2,z)\right\rangle = 0$ in Eq. (15). Thus, the element of the cross-spectral density matrix can be written as

$$\begin{aligned} & W_{jk}(\boldsymbol{r}_1,\boldsymbol{r}_2,z) \\ = & \left\langle E_{xj}^*(r_1,\varphi_1,z)E_{xk}(r_2,\varphi_2,z)\right\rangle \\ & + \left\langle E_{yj}^*(r_1,\varphi_1,z)E_{yk}(r_2,\varphi_2,z)\right\rangle. \end{aligned} \quad (16)$$

By letting $r_1 = r_2 = r$, $\varphi_1 = \varphi_2 = \varphi$ in Eq. (16) and using Eqs. (7)–(12), we can finally obtain the expressions for the intensity distribution and the degree of coherence in the focal region, respectively, as follows:[22]

$$\begin{aligned} & I_{\mathrm{t}}(r,\varphi,z) \\ = & W_{xx}(\boldsymbol{r},\boldsymbol{r},z) + W_{yy}(\boldsymbol{r},\boldsymbol{r},z) + W_{zz}(\boldsymbol{r},\boldsymbol{r},z) \\ = & I_x(r,\varphi,z) + I_y(r,\varphi,z) + I_z(r,\varphi,z), \end{aligned} \quad (17)$$

$$\begin{aligned} & \mu_{jk}(r,\varphi,z) \\ = & W_{jk}(\boldsymbol{r},\boldsymbol{r},z)/\sqrt{W_{jj}(\boldsymbol{r},\boldsymbol{r},z)W_{kk}(\boldsymbol{r},\boldsymbol{r},z)}, \\ & j,k = x,y,z. \end{aligned} \quad (18)$$

The complex degree of coherence $\mu_{jk}(r,\varphi,z)$ $(j,k = x,y,z)$ is a parameter that indicates the correlation between any two of the three orthogonal electric field components at an arbitrary point $\boldsymbol{r}$.

3. Results and discussion

To perform some numerical calculations, the coefficients $B(\theta)$ and $C(\theta)$ in Eq. (1) will be given. $B(\theta) = \cos^{-3/2}\theta$ is given for an FZP,[23] and $C(\theta)$ can be expressed as[24]

$$C(\theta) = \begin{cases} \exp[\mathrm{i}(\Delta - \delta)]\exp(\mathrm{i}\pi), & (\theta_{m-2} \le \theta \le \theta_{m-1}), \\ \exp(-\mathrm{i}\delta)\exp(\mathrm{i}\pi), & (\theta_{m-1} \le \theta \le \theta_m), \end{cases} \tag{19}$$

where $m = 2, 4, \ldots, M$, M is the total zone number, $\theta_0 = 0$, $\theta_M = \alpha$, $\delta = kf/\cos\theta - kf$, Δ is the phase difference between the two adjacent zones; θ_m is the zone angle at which zone radius is seen from the focus and defined by[23]

$$\sin\theta_m = \frac{\sqrt{m\pi(2kf + m\pi)}}{(kf + m\pi)}. \tag{20}$$

In the following investigation, it is assumed that the zone number $M = 16$ (i.e., NA is 0.996) with $\Delta = \pi$, $\omega_0 = 1$ μm and $f = 0.5$ μm.

Figure 2 shows the influence of $|E_y^0|$ on the total intensity I_t in the focal plane with $m = 1$. It can be seen that the pattern of intensity distribution changes with $|E_y^0|$. Specifically, with $|E_y^0|$ changing from $|E_y^0| = |E_x^0|$ to $|E_y^0| \neq |E_x^0|$, the pattern of I_t changes from a circular focal spot to elliptical focal spots as shown in Fig. 2(b).

Figure 3 shows the effects of varying m, NA and Δ on the total intensity distribution in the focal plane. It is found that the core intensity of the vortex beam ($m = 1$, for example) is nonzero as shown in Fig. 3(a). This is because there is a zeroth order Bessel function of the first kind, which has a maximum value near the optical axis, in the expression of $E_z(r, \varphi, z)$ for $m = 1$. On the other hand, the intensity distribution of the focused field composed of x and y components (i.e., $I_x + I_y$) has a dark core for $m = 1$. As a result, this dark hole is just filled in by the intensity of the focused field of z component, leading to the generation of a flat top beam that has many applications. The influence of varying NA on the total intensity distribution in the focal plane is presented in Fig. 3(b). It is shown that with the increase of NA, the central intensity becomes larger but the focal spot becomes smaller, indicating that the increase of NA leads to a stronger longitudinal component and a tighter focused transverse field. Figure 3(c) shows the influence of varying Δ on the total intensity distribution in the focal plane. It is found that with Δ changing from 0.5π to π, the total intensity increases. This is because when $\Delta = \pi$, the beams from the adjacent zones arrive at the focal plane exactly in phase and they interfere fully constructively there.

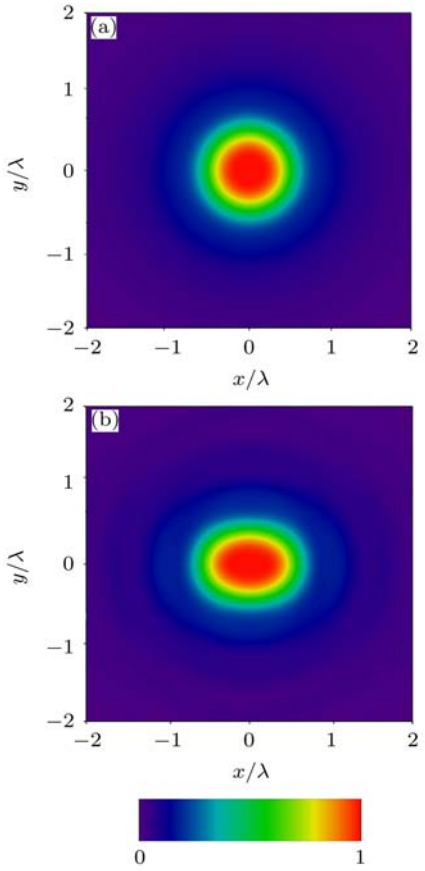

Fig. 2. (colour online) Effects of varying E_y^0 on I_t in the focal plane with $m = 1$ and $|E_y^0| = 1$ (a) and 0.75 (b). The parameters for calculation are $|E_x^0| = 1$, $\lambda = 633$ nm, $\omega_0 = 1$ μm, $f = 0.5$ μm, $\Delta = \pi$ and $M = 16$.

Now we turn to considering the modulus of the degree of coherence in the focal plane. It is interesting to discuss the degree of coherence of a partially polarized vortex beam, because the x and the y components of the partially polarized beam are completely incoherent (i.e., $|\mu_{xy}| = 0$) in the source plane. After being focused, the x and the y components of the partially polarized beam will produce their new components. Therefore, the aforementioned incoherence is expected to be improved in the focal plane. The distribution of spectral degree of coherence of a focused partially polarized vortex beam in the focal plane is illustrated in Figs. 4(a)–4(c). Since the distribution of $|\mu_{xy}|$ has not the rotation symmetry in the focal plane (i.e., Eq. (18) is related to φ), it is plotted by the contour graphics. A comparison among Figs. 4(a),

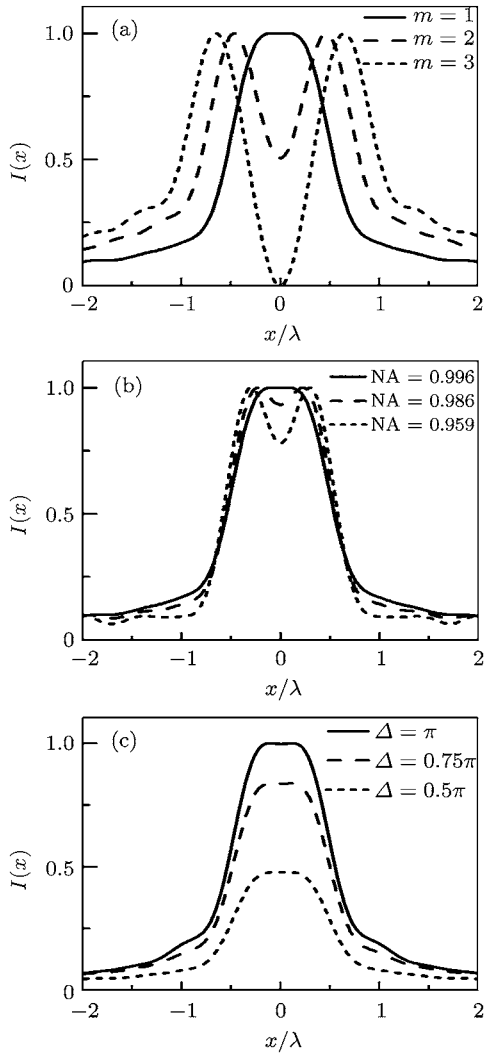

Fig. 3. Intensity distributions of a stochastic electromagnetic vortex beam in the focal plane for different values of topological charge m, numerical aperture NA and phase difference Δ. (a), (b) $\Delta = 0.5\pi$, (a), (c) NA = 0.996, $|E_y^0| = 1$. The other parameters are the same as those in Fig. 2.

4(b) and 4(c) shows that there exist high contrasts in distributions of $|\mu_{xy}|$. For instance, most of $|\mu_{xy}|$ take their minima in Fig. 4(b), but take their maxima in Figs. 4(a) and 4(c). Moreover, the patterns of $|\mu_{xy}|$ distribution are very different in the geometrical focus neighbourhood, which may be related to their different patterns of intensity distribution. Therefore, the corresponding distributions of intensity $I_x + I_y$ are plotted in Figs. 4(d)–4(f). Comparing Fig. 4(a) with Fig. 4(d), it is found that $|\mu_{xy}|$ equals zero in the bright central area. Because the electric field outside the focal spot in the focal plane is so weak that it can be considered negligible, we only need to consider the $|\mu_{xy}|$ in the geometrical focus neighbourhood. In this sense, the x and the y components of the focused field are incoherent for nonvortex beam (i.e., $m = 0$). In other words, the incoherence between the x and the y components of the electric field in the source plane is hardly changed in the focal plane for nonvortex beams. Comparing Fig. 4(b) and Fig. 4(e), it is seen that $|\mu_{xy}|$ takes its intermediate values in the area of bright ring. In Figs. 4(c) and 4(f), it is found that $|\mu_{xy}|$ is close to its lower limit in the area of bright ring, but reaches its upper limit in the secondary bright central area. It is evident that after being focused, the coherence between the x and the y components of the electric field is improved for vortex beams.

Figure 5 shows contour distributions of $|\mu_{xz}|$ and $|\mu_{yz}|$ in the focal plane for $m = 1$. It is seen that $|\mu_{xz}|$ and $|\mu_{yz}|$ are oscillating functions of (r, φ). Furthermore, it is found that there exists some relation between $|\mu_{xz}|$ and $|\mu_{yz}|$. Specifically, the pattern of $|\mu_{yz}|$ distribution can be obtained by rotating the pattern of $|\mu_{xz}|$ distribution about z axis through an angle of 90°, i.e.,

$$|\mu_{xz}(r, \varphi + \pi/2, z)| = |\mu_{yz}(r, \varphi, z)|\,. \tag{21}$$

In fact, Eq. (21) can be derived from the foregoing equations under the condition of $|E_y^0| = |E_x^0|$. Substituting $\varphi + \pi/2$ for φ in Eqs. (7)–(12), we have

$$\begin{aligned} E_{xx}(\varphi + \pi/2) &= \exp(\mathrm{i}m\pi/2)E_{yy}(\varphi), \\ E_{xz}(\varphi + \pi/2) &= -\exp(\mathrm{i}m\pi/2)E_{yz}(\varphi) \\ E_{yx}(\varphi + \pi/2) &= -\exp(\mathrm{i}m\pi/2)E_{xy}(\varphi), \\ E_{yz}(\varphi + \pi/2) &= \exp(\mathrm{i}m\pi/2)E_{xz}(\varphi), \end{aligned} \tag{22}$$

and substituting into Eq. (18), we can obtain Eq. (21).

Figure 6 shows the effects of numerical apertures of and the phase difference of binary phase FZPs on $|\mu_{xy}|$ distribution of partially polarized vortex beams in the focal plane. It is shown that the dark area, where $|\mu_{xy}|$ is close to zero, is the largest in Fig. 6(b) and is the smallest in Fig. 6(c). This indicates that the coherence between the x and the y components of the electric field can been improved by increasing the numerical aperture of binary phase FZP or reducing the phase difference of binary phase FZP from π.

Finally, we turn to considering a special case of $|E_y^0| = 0$ (i.e., the incident light beam is linearly polarized). It is found that any two of three electric field components E_x, E_y and E_z are completely coherent everywhere in the focal plane in this case, i.e.,

$$|\mu_{jk}(r, \varphi, z)| = 1, \quad (j, k = x, y, z). \tag{23}$$

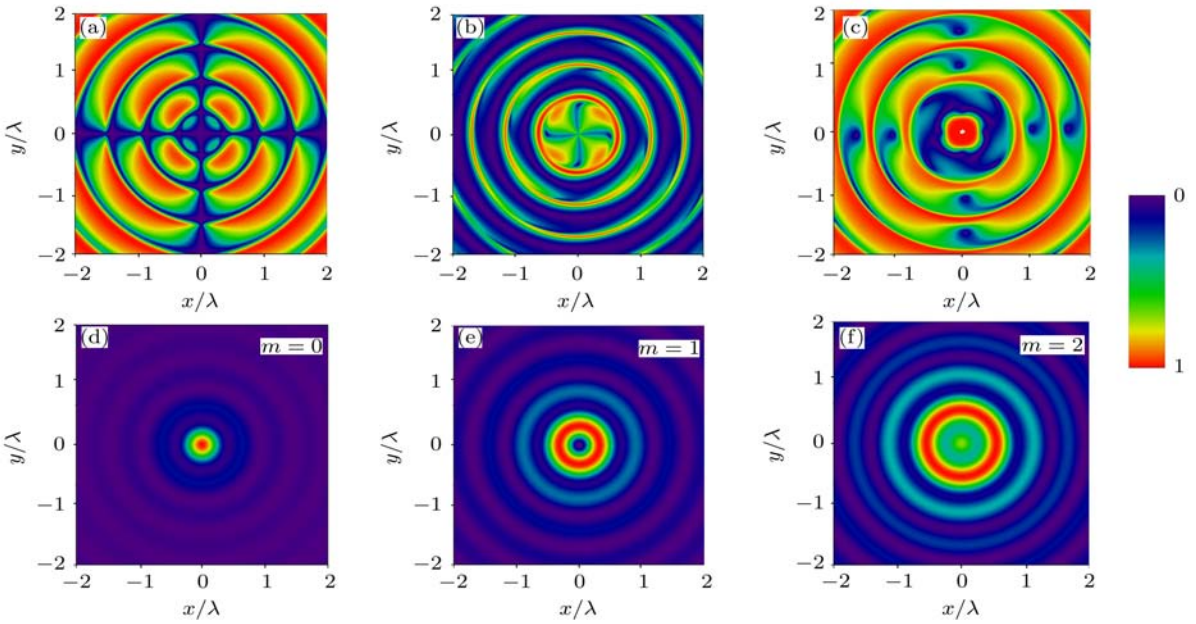

Fig. 4. (colour online) Contour distributions of $|\mu_{xy}|$ in the focal plane for different values of topological charge m and the normalized intensity distribution $I_x + I_y$ corresponding to $|\mu_{xy}|$. (a)–(c) $|\mu_{xy}|$, (d)–(f) $I_x + I_y$. (a), (d) $m = 0$, (b), (e) $m = 1$, (c), (f) $m = 2$. $\left|E_y^0\right| = 1$. The other parameters are the same as those in Fig. 2.

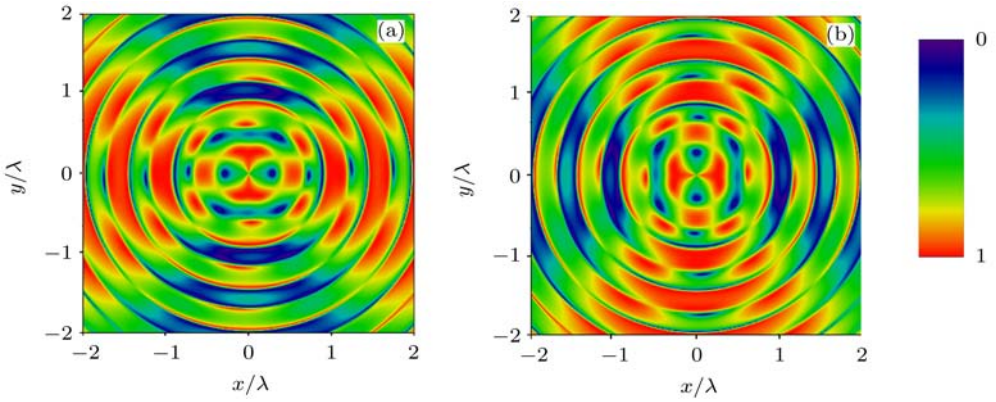

Fig. 5. (colour online) Contour distributions of $|\mu_{xz}|$ and $|\mu_{yz}|$ in the focal plane for $m = 1$. (a) $|\mu_{xz}|$, (b) $|\mu_{yz}|$, $\left|E_y^0\right| = 1$. The other parameters are the same as those in Fig. 2.

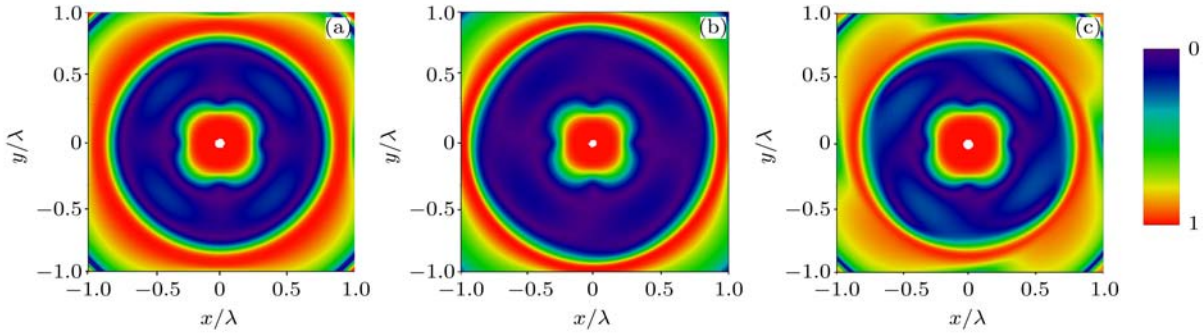

Fig. 6. (colour online) Effects of NA and Δ on $\left|\mu_{jk}\right|$ distribution of partially polarized vortex beams in the focal plane. $m = 2$, $\left|E_y^0\right| = 1$. (a) $\Delta = \pi$, NA=0.996. (b) $\Delta = \pi$, NA=0.959. (a) $\Delta = 0.2\pi$, NA=0.996. The other parameters are the same as those in Fig. 2.

Substituting $\left|E_y^0\right| = 0$ into Eq. (3), we obtain

$$E_{yj}(r, \varphi, z) = 0, \quad (j = x, y, z). \tag{24}$$

Substituting this into Eqs. (16) and (18), we have

$$|\mu_{jk}(r,\varphi,z)| = \frac{\left|\left\langle E^*_{xj}(r,\varphi,z)E_{xk}(r,\varphi,z)\right\rangle\right|}{\sqrt{\left\langle E^*_{xj}(r,\varphi,z)E_{xj}(r,\varphi,z)\right\rangle\left\langle E^*_{xk}(r,\varphi,z)E_{xk}(r,\varphi,z)\right\rangle}} = \frac{\left|E^*_{xj}(r,\varphi,z)E_{xk}(r,\varphi,z)\right|}{\sqrt{\left(E^*_{xj}(r,\varphi,z)E_{xk}(r,\varphi,z)\right)\left(E^*_{xk}(r,\varphi,z)E_{xj}(r,\varphi,z)\right)}}.$$

According to Eqs. (4) and (5), the calculations of $E_{xk}(r,\varphi,z)$ and $E_{xj}(r,\varphi,z)$ are independent. Thus, we have

$$|\mu_{jk}(r,\varphi,z)| = \frac{\left|E^*_{xj}(r,\varphi,z)E_{xk}(r,\varphi,z)\right|}{\sqrt{\left(E^*_{xj}(r,\varphi,z)E_{xk}(r,\varphi,z)\right)\left(E^*_{xj}(r,\varphi,z)E_{xk}(r,\varphi,z)\right)^*}} = \frac{\left|E^*_{xj}(r,\varphi,z)E_{xk}(r,\varphi,z)\right|}{\sqrt{\left|E^*_{xj}(r,\varphi,z)E_{xk}(r,\varphi,z)\right|^2}} = 1.$$

That is exactly Eq. (23), the equation we set out to prove.

4. Conclusion

We derive the expression for the electric field of the tightly focused partially polarized vortex beam according to the vectorial Debye theory. The effects of the numerical apertures of and phase difference of binary phase FZPs, the topological charges of vortex beam, and the degree of polarization of incident beam on the intensity distribution and spectral degree of coherence in the focal region are investigated in great detail. It is shown that elliptical light spots can be obtained in the focal plane by selecting properly the degree of polarization of the incident beam and a flat top beam can be obtained in the focal plane when the topological charge of the vortex beam $m = 1$. The two special intensity distributions have wide applications. Studies of degree of coherence reveal that the degree of coherence between x and y components of the electric field, which is zero in the source plane, is improved in the focal plane for vortex beam, but it is hardly changed for nonvortex beam. Moreover, it is found that the pattern of $|\mu_{yz}|$ distribution can be obtained by rotating the pattern of $|\mu_{xz}|$ distribution about z axis through an angle of 90° if the high NA phase FZP is illuminated by natural light. Finally, it is proved that any two of the three electric field components E_x, E_y and E_z are completely coherent everywhere in the focal plane if the incident light beam is linearly polarized, which indicates that a linearly polarized beam will not become a partially polarized beam by resolving it into two orthogonal components in practical applications.

References

[1] Rydberg C 2008 *Opt. Lett.* **33** 104
[2] Foreman M R and Torok P 2009 *J. Opt. Soc. Am.* A **26** 2470
[3] Bokor N and Davidson N 2007 *Opt. Commun.* **279** 229
[4] Du Y G, Han Y P, Han G X and Li J J 2011 *Acta Phys. Sin.* **60** 028702 (in Chinese)
[5] Walker E P and Milster T D 2001 *Proc. SPIE* **4443** 73
[6] Helseth L E 2002 *Opt. Commun.* **212** 343
[7] Hua L M, Chen B S, Chen Z Y and Pu J X 2011 *Chin. Phys.* B **20** 358
[8] Zhan Q and Leger R J 2002 *Opt. Express* **10** 324
[9] Zhang Z M, Pu J X and Wang X Q 2008 *Appl. Opt.* **47** 1963
[10] Yu Y J, Chen J N, Yan J L and Wang F F 2011 *Acta Phys. Sin.* **60** 230 (in Chinese)
[11] Allen L, Beijersbergen M W, Spreeuw R J C and Woerdman J P 1992 *Phys. Rev.* A **45** 8185
[12] Allen L and Padgett M J 2000 *Opt. Commun.* **184** 67
[13] Terriza G M, Torres J P and Torner L 2003 *Opt. Commun.* **228** 155
[14] Roux F S 2004 *Opt. Commun.* **242** 45
[15] Gibson G, Courtial J, Padgett M J, Vasnetsov M, Pas'ko V, Barnett S M and Franke-Arnold S 2004 *Opt. Express* **12** 5448
[16] Zhao Y, Edgar J S, Jeffries G D M, McGloin D and Chiu D T 2007 *Phys. Rev. Lett.* **99** 073901
[17] Wieland M, Frueke R, Wilhein T, Spielmann C, Pohl M and Kleineberg U 2002 *Appl. Phys. Lett.* **81** 2520
[18] Carnal O, Sigel M, Sleator T, Takuma H and Mlynek J 1991 *Phys. Rev. Lett.* **67** 3231
[19] Doak R B, Grisenti R E, Rehbein S, Schmahl G, Toennies J P and Wöll Ch 1999 *Phys. Rev. Lett.* **83** 4229
[20] Wolf E 1959 *Proc. R. Soc. London,* Ser. A **253** 349
[21] Gu M 1999 *Advanced Optical Imaging Theory* (Belin: Springer-Verlag)
[22] Setälä T, Shevchenko A, Kaivola M and Friberg A T 2002 *Phys. Rev.* E **66** 016615
[23] Lindfors K, Setala T, Kaivola M and Friberg A T 2005 *J. Opt. Soc. Am.* A **22** 561
[24] Kalosha V P and Golub I 2007 *Opt. Lett.* **32** 3540
[25] Mote R G, Yu S F, Zhou W and Li X F 2009 *Appl. Phys. Lett.* **95** 191113